



1 **Recent evolution and associated hydrological dynamics of a vanishing Tropical Andean**
2 **glacier: *Glaciar de Conejeras*, Colombia**

3

4 Enrique Morán-Tejada¹, Jorge Luis Ceballos², Katherine Peña², Jorge Lorenzo-Lacruz¹ and
5 Juan Ignacio López-Moreno³

6

- 7 1. Department of Geography. University of the Balearic Islands. Palma, Spain
8 2. Instituto de Hidrología, Meteorología y Estudios Ambientales (IDEAM). Bogotá, Colombia
9 3. Pyrenean Institute of Ecology. Consejo Superior de Investigaciones Científicas. Zaragoza, Spain.

10

11

12 **Abstract**

13 Glaciers in the inner tropics are rapidly retreating due to atmospheric warming. In Colombia, this
14 retreat is accelerated by volcanic activity, and most glaciers are in their last stages of existence.
15 There is general concern about the hydrological implications of receding glaciers, as they
16 constitute important freshwater reservoirs and, after an initial increase in melting flows due to
17 glacier retreat, a decrease in water resources is expected in the long term as glaciers become
18 smaller. In this paper, we perform a comprehensive study of the evolution of a small Colombian
19 glacier, Conejeras (Parque Nacional Natural de los Nevados), that has been monitored since
20 2006, with special focus on the hydrological response of the glacierized catchment. The glacier
21 shows great sensitivity to changes in temperature and especially to the evolution of the ENSO
22 phenomenon, with great loss of mass and area during El Niño warm events. Since 2006 it has
23 suffered a 37% reduction from 22.45 ha to 12 ha in 2017, with an especially abrupt reduction
24 since 2014. During the period of hydrological monitoring (June 2013 to December 2017)
25 streamflows at the outlet of the catchment experienced a noticeable cycle of increasing flows up
26 to mid-2016 and decreasing flows afterwards. The same kind of cycle was observed for other
27 hydrological indicators, such as slope of the rising flow limb or the monthly variability of flows. We
28 observed an evident change in the daily hydrograph: from a predominance of days with a pure
29 melt-driven hydrograph up to mid-2016, to an increase in the frequency of days with flows less
30 influenced by melt after 2016. Such a hydrological cycle is not directly related to fluctuations of
31 temperature or precipitation; therefore, it is reasonable to consider that it is the response of the
32 glacierized catchment to retreat of the glacier. Results confirm the necessity for small-scale
33 studies at a high temporal resolution in order to understand the hydrological response of glacier-
34 covered catchments to glacier retreat and imminent glacier extinction.

35

36

37 **Key words:** glacier retreat, melting flows, tropical glaciers; hydrological change; tipping point

38

39

40

41

42

43

44

45

46

47



48 **1. Introduction**

49 **1.2 Andean glaciers and water resources**

50 Glacier retreat is one the most prominent signals of global warming; glaciers from most mountain
51 regions in the world are disappearing or have already disappeared due to atmospheric warming
52 (Vaughan et al., 2013). Of the retreating mountain glaciers worldwide, those located within the
53 tropics are particularly sensitive to atmospheric warming (Chevallier et al., 2011; Kaser and
54 Omaston, 2002). Their locations in the tropical region involve a larger energy forcing in terms of
55 received solar radiation compared to other latitudes. Unlike glaciers in mid and high latitudes,
56 subject to freezing temperatures during a sustained season, tropical glaciers may experience
57 above-zero temperatures all year round, especially at the lowest elevations, involving constant
58 ablation and rapid response of the glacier snout to climate variability and climate change (Francou
59 et al., 2004; Rabatel et al., 2013). As a result of atmospheric warming since mid-20th century,
60 glaciers in the tropics are seriously threatened, and many of them have already disappeared
61 (Vuille et al., 2008). Of the tropical glaciers, 99% are located in the Central Andes and constitute
62 a laboratory for glaciology (see review in Vuille et al., 2017), including studies regarding glaciers'
63 response to climate forcing (e.g. Favier et al., 2004; Francou et al., 2004, 2003; López-Moreno et
64 al., 2014), and regarding hydrological and geomorphological consequences of glacier retreat
65 (Bradley et al., 2006; Chevallier et al., 2011; Kaser et al., 2010; López-Moreno et al., 2017;
66 Ribstein et al., 1995; Sicart et al., 2011), and also regarding the vulnerability of populations to
67 risks associated with glacier retreat (Mark et al., 2017). Perhaps the glaciers in the most critical
68 situation in the Andean mountains are those located in the inner tropics, including the countries
69 of Ecuador, Venezuela and Colombia. In the latter, a constant deglaciation since the 1970s has
70 been reported, with an acceleration since the 2000s (Ceballos et al., 2006; Rabatel et al., 2013),
71 and most glaciers are in danger of disappearing in the coming years (Poveda and Pineda, 2009;
72 Rabatel et al., 2017). In the outer tropics, the variability of glacier mass balance is highly
73 dependent on seasonal precipitation; thus, during the wet season (December-February) freezing
74 temperatures ensure seasonal snow cover that increases the glaciers' surface albedo and
75 compensates mass balance losses of the dry season. In contrast, for glaciers of the inner tropics,
76 ablation rates remain more or less constant throughout the year due to the absence of seasonal
77 fluctuations of temperature and to a freezing level which is constantly oscillating within the
78 glaciers' elevation ranges. Therefore, the mass balance of these glaciers is more sensitive to
79 inter-annual variations of temperature; hence they are much more sensitive to climate warming
80 (Ceballos et al., 2006; Favier et al., 2004; Francou et al., 2004; Rabatel et al., 2013, 2017). In
81 Colombia, this situation is further aggravated by the location of glaciers near or on the top of
82 active volcanos. The hot pyroclastic material emitted during volcanic eruptions and the reduced
83 albedo of glaciers' surface by the deposition of volcanic ash, have notably contributed to rapid
84 deglaciation in these areas (Huggel et al., 2007; Rabatel et al., 2013; Vuille et al., 2017).

85 Regardless of the loss of natural scientific laboratories (Francou et al., 2003) of landscape and
86 cultural emblems of mountainous areas (IDEAM, 2012; Rabatel et al., 2017), the vanishing of
87 glaciers has a major impact on livelihoods of communities living downstream, including potential
88 reduction of freshwater storage and changes in the seasonal patterns of water supply by
89 downstream rivers (Kaser et al., 2010). Glaciers constitute natural water reservoirs in the form of
90 ice accumulated during cold and wet seasons, and they provide water when ice melts during
91 above-freezing temperature seasons. The hydrological importance of glaciers for downstream
92 territories depends on the availability of other sources of runoff, including snow melt and rainfall.
93 Therefore, water supply by glaciers becomes critical for arid or semi-arid regions downstream of
94 the glaciated areas, buffering the lack of sustained precipitation or water provided by seasonal
95 melt of snow cover (Rabatel et al., 2013; Vuille et al., 2008). Such is the case for the western
96 slopes of the tropical Andes: in countries like Peru or Bolivia, with a high variability in precipitation
97 and a sustained dry season, the contribution of glacier melt is crucial for socioeconomic activities
98 and for water supply, especially since it is one of the main sources of water for the highly
99 populated capital cities of Lima and La Paz (Kaser et al., 2010; López-Moreno et al., 2014; Soruco
100 et al., 2015; Vuille et al., 2017). In more humid/temperate regions (i.e. the Alps or western North
101 America) the melt of seasonal snow cover provides the majority of water during the melt season
102 (Beniston, 2012; Stewart et al., 2004) and glacier melt is a secondary contributor. However, even
103 in this region, water availability can be subject to climate variability, and the occurrence of dry and



104 warm periods that comprise thin and brief snow cover may involve glacier melt as the main
105 source of water during such events (Kaser et al., 2010). In the inner tropics, glaciers may not
106 constitute the main source of water for downstream populations, as the seasonal shift of the
107 Intertropical Convergence Zone (Poveda et al., 2006) assures two humid seasons every year;
108 however, the loss of water from glacier melt can affect the eco-hydrological functioning of the
109 wetland ecosystems called “*páramos*”, which are located in the altitudinal tier located below that
110 of the periglacial ecosystem (Rabatel et al., 2017). Agriculture and livestock in Colombian
111 mountain communities are partly dependent on water from these important water reservoirs that
112 provide constant water flow to downstream rivers even during periods of less precipitation.
113

114 1.2. Hypothesis and objectives

115 The present work is focused on the hydrological dynamics of a Colombian glacier near extinction
116 due to prolonged deglaciation. Hock et al. (2005) presented a summary of the effects of glaciers
117 on streamflow compared to unglaciated areas. The main characteristics of streamflow can be
118 summarized as follows (Hock et al., 2005):

- 119 - Specific runoff dependence on variability of glacier mass balance. In years of mass
120 balance loss, total streamflow will increase as water is released from glacier storage. The
121 opposite will happen in years of positive mass balance.
- 122 - Seasonal runoff variation dependent on ablation and accumulation periods at latitudes
123 with markedly variable temperature and/or precipitation seasonal patterns. This does not
124 apply to glaciers in the inner tropics
- 125 - Large diurnal fluctuation in the absence of precipitation as a result of the daily cycle of
126 temperature and derived glacier melt.
- 127 - Moderation of year-to-year variability. Moderate percentages (10 to 40%) of ice cover
128 fraction within the basin reduces variability to a minimum, but it becomes greater at both
129 higher and lower glacierization levels.
- 130 - Large glacierization involves a high correlation between runoff and temperature, whereas
131 low levels of glacier cover increase runoff correlation with precipitation.

132 However, under warming conditions that lead to glacier retreat, the hydrological contribution of
133 the glacier may notably change from the aforementioned characteristics. The retreat of a glacier
134 is a consequence of prolonged periods of negative mass balance, the result of a disequilibrium
135 in the accumulation/ablation ratio that involves an upward shift of the equilibrium line (the
136 elevation at which accumulation and ablation volumes are equal), and an increase of the ablation
137 area with respect to the accumulation area (Chevallier et al., 2011). As a result, the glaciated area
138 is increasingly smaller compared to the non-glaciated area within the catchment in which the
139 glacier is settled. Under such conditions of sustained negative mass balance, the hydrological
140 response of the glacier will be a matter of time-scales (Chevallier et al., 2011; Hock et al.,
141 2005). The total runoff production of the retreating glacier comprises a tradeoff between two
142 processes: on one side, an acceleration of glacier melt that will increase the volume of glacier
143 outflows independent of the volume precipitated as snowfall or rainfall; on the other side, water
144 discharges from the catchment decrease because the water reservoir that represents the glacier
145 is progressively emptying (Huss and Hock, 2018). Thus, the contribution of glacier melt to total
146 water discharge will initially increase, as the first process will dominate over the other; however,
147 after reaching a discharge peak, the second process dominates, leading to a decrease in water
148 discharge until the glacier vanishes. In terms of runoff variability, there is also a different signal
149 between initial and final stages of glacier retreat: on a daily basis, the typical diurnal cycle of
150 glacier melt will exacerbate at the initial stages (larger difference between peak and base runoff)
151 and will moderate at the final stages. However, in terms of year-to-year variability, there can be
152 a reduction or increase at the initial stages, depending on the original glaciated area, and an
153 increase in the long term, as the water yield will correlate with precipitation instead of temperature
154 because the percentage of runoff from glacier melt decreases with decreasing glacierization
155 (Hock et al., 2005).

156 The objective of the present work is to provide a comprehensive analysis of the hydrological
157 dynamics of a glaciated basin, with the glacier in its last stages prior to extinction. Thanks to sub-
158 hourly meteorological and hydrological data, changes in time of streamflow dynamics as a result



159 of changes in atmospheric conditions and/or changes in the glacier area resulting from mass
160 balance loss are also explored. Results can be representative of expected hydrological dynamics
161 in other glaciated areas in the Andes, with glaciers close to extinction.

162

163 2. Study site

164 Our study focuses on the Conejeras glacier, a very small ice mass (14 hectares in 2017) that
165 forms part of a larger glacier system called Nevado de Santa Isabel (1.8 km²), one of the six
166 glaciers that still persist in Colombia. It is located in the Cordillera Central (the central range of
167 the three branches of the Andean chain in Colombia) and, together with the glaciers of Nevado
168 del Ruiz and Tolima, comprises the protected area called Parque Nacional Natural de los
169 Nevados (Fig. 1). The summit of the Santa Isabel glacier reaches 5100 m, being the lowest glacier
170 in Colombia. As a result, it is as well the most sensitive to atmospheric warming and why it has
171 been monitored since 2006, part of the world network of glacier monitoring (IDEAM, 2012). The
172 Santa Isabel glacier has been retreating since the 19th century, with an intensification of
173 deglaciation since the middle of the 20th century. As a result, the glacier is now a set of separated
174 ice fragments instead of a continuous ice mass, as it was a decade ago (IDEAM, 2012). One of
175 the fragments, located at the north-east sector of the glacier, is the Conejeras glacier, which is
176 the object of this study, whose elevation ranges between 4700 and 4895 m. In 2006, at the glacier
177 terminus, hydro-meteorological stations were installed in order to measure glacier contribution to
178 runoff, as well as air temperature and precipitation.

179 The Conejeras water stream is a tributary of one of the “quebradas” (Spanish name for small
180 mountain rivers in South American countries) flowing into the river Rio Claro. Thus, the Conejeras
181 glacier corresponds to the uppermost headwaters of the Rio Claro basin (Fig. 1). The Rio Claro
182 basin comprises an elevation range of (2700 to 4895 m) and, from higher to lowest, presents a
183 succession of typical Andean ecosystems: glacial (4700 to 4894), periglacial (4300 – 4700 m),
184 páramo wetland ecosystem (3600 to 4300 m) and high elevation tropical forest *bosque altoandino*
185 (2700 to 3600 m). Mean annual temperature at the glacier base is $1.3 \pm 0.7^\circ\text{C}$, with very little
186 seasonal variation, and precipitation sums reach 1025 ± 50 mm annually, with two contrasted
187 seasons (see Figure 2), resulting from the seasonal migration of the Intertropical Convergence
188 Zone (ITCZ, Poveda et al., 2006). During the dry season (December to January and June to
189 August), mean precipitation barely reaches 75 mm per month, whereas during the wet season
190 (March to May and September to October), values exceed 150 mm per month.

191

192

193

194

195 3. Data and Methods

196

197 3.1. Hydrological and meteorological data

198 Meteorological and hydrological data used in the present work has been collected by the Institute
199 for Hydrological, Meteorological and Environmental Studies of Colombia (IDEAM, *Instituto de*
200 *Hidrología, Meteorología y Estudios Ambientales*), thanks to the automatic meteorological and
201 gauge stations network at the Río Claro basin.

202 The experimental site of the Río Claro basin has been monitored since 2009, with a network of
203 meteorological and hydrological stations consecutively located at the tributaries of the Río Claro
204 river, covering an altitudinal gradient of 2700 – 4900 m.asl. For the present study, data was used
205 from stations located at the Conejeras glacier surroundings, including: 15-minute resolution water
206 yield (m³ s⁻¹), hourly temperature (°C) (both stations located at 4662 m.asl) and 10-minute
207 precipitation (mm, the station located at 4413 m. asl). Even though these data have been available
208 since 2009, quality analysis prevented us from using the entire series, as numerous
209 inhomogeneities, out-of-range values and empty records were present. From 2013 automatic
210 sensors stabilized and data is suitable for analysis. The period covered for analysis ranges from
211 June 2013 to December 2017, a total of 56 months, and data was aggregated hourly, daily and



212 monthly to perform statistical analyses. However, in order to obtain a wider perspective, and to
213 take advantage of the effort made by the glaciologist of IDEAM for conscientiously undertaking
214 mass balance measurements every month since 2006, also shown are trends and variability in
215 climate (from nearby meteorological stations of the Colombian national network) and glacier mass
216 evolution for the longest time period available. The Multivariate ENSO Index, used for
217 characterizing influence of the ENSO phenomenon on the glacier evolution, has been
218 downloaded from NOAA <https://www.esrl.noaa.gov/psd/enso/mei/table.html> (December 2017).

219

220 3.2. Glacier evolution data

221 The evolution of the Conejeras glacier (Fig. 3) has been monitored by the Department of
222 Ecosystems of IDEAM. Since March 2006, a network of 14 stakes was installed on the Conejeras
223 glacier to measure ablation and accumulation area. The 6–12 m long stakes are PVC pipes of 2
224 m length. These 14 stakes are vertically inserted into the glacier at a depth not less than five
225 meters and they are roughly organized in 6 cross profiles at about 4670, 4700, 4750, 4780, 4830
226 and 4885 m a.s.l. Accumulation and ablation measurements are performed monthly. Typical
227 measurements of the field surveys include stake readings (monthly), density measurement in
228 snow and firn pits (once per year), and re-drilling of stakes (if required) to the former position. The
229 entire methodology can be found in (Mölg et al., 2017; Rabatel et al., 2017). The mass balance
230 data is calculated with the classical glaciological method that represents the water equivalent that
231 glacier gains or losses in a given time. This data is used to generate yearly mappings of mass
232 balance and calculate the equilibrium line altitude (ELA), which is the altitude point where mass
233 balance is equal to zero equivalent meters of water, and separates the ablation and accumulation
234 area in the glacier (Francou and Pouyaud, 2004).

235

236 Changes in glacier surface have been measured by direct topographic surveys (in the years 2009,
237 2012, 2014, and 2017) or computed using satellite imagery (Landsat and Sentinel constellations)
238 for the other years within the 2006–2018 period. Free-cloud cover Landsat TM images were
239 selected until 2011 and then Landsat OLI or Sentinel 2 images were selected when data became
240 available. A set of 8 images was processed in order to support direct topographic surveys for ice-
241 covered area measurements. TOA (Top Of Atmosphere) Reflectance was obtained using specific
242 radiometric calibration coefficients for each image and sensor (Chander et al., 2009; Padró et al.,
243 2017). BOA (Bottom of the Atmosphere) Reflectance was based on the Dark Object Subtraction
244 (DOS) approach (Chavez, 1988). The Normalized Difference Snow Index (NDSI) was used to
245 discriminate snow and ice covered areas from snow-free areas. The NDSI is expressed as the
246 relationship between reflectance in the visible region and reflectance in the medium-infrared
247 region (the specific bands vary among different sensors; e.g. TM bands 2 and 5). Pixels in the
248 different images were classified as snow- or ice- covered areas when the NDSI was greater than
249 0.4 (Dozier, 1989).

250

251

252 3.3. Statistical Analyses

253 A number of indices were extracted from the streamflow, temperature and precipitation hourly
254 series in order to assess changes in time in the hydrological output of the glacier and their relation
255 to climate (Table 1). These daily indices were subject to statistical analyses including correlation
256 tests, monthly aggregation and assessment of changes on time.

257 Since one of the main objectives of the paper is to characterize daily dynamics of streamflow and
258 changes in time, a principal component analysis (PCA) was conducted in order to extract the
259 main patterns of daily streamflow cycles. The data matrix for the PCA was then composed by
260 streamflow hourly values in 1614 columns as variables (number of days) and 24 rows as cases
261 (hours in a day). As the PCA does not allow the number of variables to exceed the number of
262 cases, PCAs were performed on 25 bootstrapped random samples of days ($n=23$, with
263 replacement); it was ensured that results with three principal components were stable throughout
264 the samples (see table 3 in results sections). After the main PCs were extracted, calculation of
265 correlation between each day of the time series and the selected PCs was determined. The PC
266 that best correlated with the correspondent day was assigned to every day, obtaining a time-



267 series of the three PCs. This allowed assessment of changes in time of the main patterns of daily
268 streamflow cycles observed.

269

270 4. Results

271 4.1. Climatology and glacier's evolution

272 The long-term climatic evolution of the study area is depicted in Figure 2. The temperature and
273 precipitation series (Fig. 2 a, c and d) correspond to the Brisas meteorological station, which is
274 located 25 km from the glacier, at 2721 m elevation. It therefore does not accurately represent
275 the climate conditions at the glacier, especially due to the lapse rate of temperature with elevation
276 (which makes temperatures at the glacier 3.2 °C lower: annual mean temperature of 1.4 °C at the
277 glacier's base, compared to 4.6 °C at Brisas). It is, however, the closest meteorological station
278 with available meteorological data to study long-term climate.

279 Long-term evolution of temperature does not show any significant trend or pattern from 1982 to
280 2015; however, a spectral analysis shows that the frequency with higher spectral density
281 corresponds with a seasonality of 48 months, indicating a recurrent cycle every 4 years. By
282 comparing Fig. 2a with Fig. 2b we observe a close match between temperature and evolution of
283 the Multivariate ENSO Index ($R = 0.49$), which shows, as well, a high value of power spectra in
284 the 48-month frequency cycle. Notwithstanding other factors whose analysis is far beyond the
285 scope of this paper, it is evident that the evolution of temperature in the study area is highly driven
286 by the ENSO phenomenon. Regarding precipitation (Fig. 2c), no long-term trend is observed, and
287 the most evident pattern is the bi-modal seasonal regime (Fig. 2d) with two "humid" seasons and
288 two "dry" seasons every year, typical of the whole country that is driven by a seasonal shifting of
289 the Intertropical Convergence Zone (ITZC).

290

291 The evolution of the glacier since 2006 is shown in Figure 3. Almost every month since
292 measurements began in 2006, the glacier has lost mass (113 months), and very few months (20)
293 saw a positive mass balance was recorded. The global balance in this period is a loss of 34.4
294 meters of water equivalent. For the sake of visual comparison, the mass balance evolution in the
295 temperature and MEI plot's (Fig. 2a and 2b) are included, and the close correspondence between
296 the variables is observed. During the warm phases of ENSO (Niño events, values of MEI above
297 0.5) the glacier loses up to 600 mm w.e. per month, as in the Niño event of 2009-2010, when the
298 glacier lost a total of 7000 mm w.e. One could surmise that during La Niña (cold phases of ENSO,
299 MEI values < -0.5) the glacier could recuperate mass. In fact, when MEI values are negative, the
300 glacier experiences much less decrease; however, even during the strongest La Niña events, the
301 balance is negative, with just a few months having a positive balance (e.g. in the 2010-2011 La
302 Niña, the glacier lost 1000 mm w.e.) This occurs because even during La Niña mean
303 temperatures at the glacier are above zero (0.8 ± 0.3 °C). The aforementioned agreement
304 between ENSO and mass balance appears to break from 2012 onwards. There were two events
305 of large mass balance loss around 2013-2014 that do not match with El Niño events, but they do
306 coincide with temperature peaks. This might be due to other factors that affect temperature and
307 mass balance such as increasing radiation due to less cloudiness. But some peaks of mass
308 balance loss that do not correspond to temperature peaks were also observed. A local factor
309 that can affect the glacier's mass balance independently of climatology is the quantity of deposited
310 ash on the ice surface that comes from the nearby Santa Isabel volcano. This variable has not
311 been considered in the present study but could be the subject of further research, since a
312 meteorological station that includes albedo measurements has been recently installed on the top
313 of the glacier.

314 In terms of the glacier's area, there has been a 37% reduction, from 22.45 ha in 2006 to 12 ha in
315 2017. However, this reduction has been far from linear. Between 2006 and 2014 the area
316 reduction was 9%, occurring in a gradual fashion, and one year (2012) saw a slight recuperation
317 in glaciated area. Reduction during these years was limited to a slight receding of the glacier's
318 snout, and no apparent changes were observed in the upper parts of the ice body (see map in
319 Figure 3). From 2014 to 2017, in contrast, there has been a sharp decrease in the glacier's area,



320 being especially drastic between 2014 and 2015, with substantial receding of the snout combined
321 with a retreat of ice in the upper parts of the glacier.

322

323

324 4.2. Hydrological dynamics

325 The water yield of the Conejeras glacier is measured at a gauge station located 300 m from the
326 glacier snout (when the station was installed in 2009, it was only 10 meters away from the glacier
327 snout). The water volume measured at this station is a combination of water from glacier melt and
328 water from precipitation into the watershed area, although the former exerts a larger control in
329 water yield variability. Table 2 shows the correlation between hydrological and temperature
330 indices for samples of days with precipitation, independent of the amount of fallen precipitation
331 (left), and for samples of days without precipitation (right). On days without precipitation, most
332 hydrological indices show significant correlation with temperature, except for Q_{base} and hQ_{max} .
333 The highest correlation values are found between Q_{max} , Q_{range} , Q_{slope} and $totalQ$, with T_{max}
334 and T_{med} (correlation values in the range of 0.5 – 0.65), indicating that the higher the
335 temperatures, the more prominent the melting pulse of runoff. T_{min} shows smaller and less
336 significant correlation values. The $hpulse$ also shows high correlation with temperature, but in this
337 case in a negative fashion, indicating a later occurrence of the daily melting pulse when minimum
338 temperatures and maximum temperatures are lower. On days with precipitation, correlation
339 values are generally smaller but in some cases, still significant as for Q_{max} , Q_{range} and Q_{slope} .

340 A Principal Component Analysis (PCA) performed on hourly streamflow data (in a recursive
341 fashion, see section 3.3 for explanation of the method) allowed procurement of the main patterns
342 of daily flow, as well as the changes in time during the study period. Three principal components
343 were obtained, whose values of explained variance were stable throughout the 25 bootstrapped
344 samples (Table 3). The first PC explained an average of $48 \pm 6\%$ of the variance throughout the
345 25 samples, and the second PC an average of $35 \pm 5.7\%$. Together they account for 83% of
346 variance and they both showed a neat pattern of daily streamflows (Fig. 4a). The main difference
347 between PC1 and PC2 is the time of the day when peak flows are reached and hence the time
348 range when most daily flows occur. Thus, PC1 corresponds to days with an earlier melt pulse
349 (towards 10 am) and earlier peak flows (towards 14h), compared to PC2, with days of melt pulse
350 at 13h and peak flows at 18h. The remaining PC explains a residual percentage of the variance
351 and, unlike PC1 and PC2, does not show a stable streamflow pattern across the samples.
352 However, it was decided to keep it, as it can help explain some peculiarities in the results. In
353 Figure 4b the evolution of the frequency (days per month) of days corresponding to each PC is
354 shown. Although there is some degree of variability, the frequency of days with PC1 streamflow
355 pattern increases over time, and dominates over the frequency of PC2 and PC3 days. This is
356 especially significant between 2015 and 2016, coinciding with an El Niño event. However, by mid-
357 2016 the frequency of PC1 days drops considerably and the frequency of PC2 days increases in
358 the same ratio. Thus, from mid-2016 to the end of the study period, they both maintain similar
359 levels of frequency.

360 In order to understand the underlying factors of each PC, the frequency distributions of the climatic
361 and hydrological indices for the days corresponding to each PC was computed, in the form of
362 boxplots (Figure 5). From a hydrological point of view, PC1 better corresponds to days with higher
363 total runoff and maximum runoff and with a more pronounced slope in both the rising and
364 decreasing limbs of the peak flow volume than PC2 and PC3. The variability (expressed by the
365 amplitude of boxes in the boxplots) of such hydrological indicators is, as well, higher amongst
366 days of PC1, compared to days of PC2 and PC3. Base runoff is higher in PC1 but not significantly.
367 The contrasted weight of climate may explain such hydrological differences between PCs: days
368 of PC1 present significantly higher mean temperature (median = 1.7°C) and maximum
369 temperature (median = 3.8°C) than days of PC2 (0.9°C and 2.4°C respectively) and PC3 (0.5°C
370 and 1.6°C respectively). In contrast, precipitation is notably higher (and shows greater variability)
371 in days grouped within PC3 (median = 2.2 mm day^{-1}) and PC2 (1.9 mm day^{-1}) compared to
372 days of PC1 (0.3 mm day^{-1}). To summarize, PC1 corresponds to a daily regime of pure glacier
373 melting, whereas PC2 and PC3 correspond to days with a lower glacier melting pulse with more
374 (PC3) or less (PC2) influence of precipitation.



375

376

377

378 In Figure 4 a notable change occurs in the frequency of the two main patterns of hourly
379 streamflow, PC1 and PC2, by mid-2016. Further details regarding changes in the hydrological
380 yield of the glacier are shown in Figure 6, which presents the evolution of the main hydrological
381 indices computed, along with temperature, precipitation and glacier mass balance, during the
382 study period and averaged monthly. Total and maximum daily streamflow ($totalQ$ and Q_{max})
383 depict an increasing trend up to mid-2016, where they begin to decrease. During the last 18
384 months, they remain at low levels compared to previous months. This turning point seems to
385 coincide in time with the 2015-16 El Niño event, with higher-than-average temperatures and low
386 levels of precipitation that led to an increasing mass balance loss and therefore increased flows.
387 Similar evolution is observed in the difference between base flows and maximum flows (Q_{range}),
388 as well as the slope of the rising limb of diurnal flows (Q_{slope}) which are indicators of diurnal
389 variability: they increase up to 2016 and decrease afterwards, which coincides with the change in
390 the frequency of daily streamflow patterns in Fig. 5. The mean hour of the day at which maximum
391 flows are reached (hQ_{max}) shows a steady evolution until mid-2016 when it begins to rise. This
392 seems surprising when comparing it to the evolution of hT_{max} (i.e. the hour of the day when
393 maximum temperature is reached) which does not show any particular trend. Regarding the
394 monthly variability of flows (third panel on the right, Fig. 7) we observe the same turning point with
395 a clear decrease in the coefficient of variation until 2016 and an increase afterwards. It is clear
396 that a hydrological change has occurred at the outlet of the glacier, but when we look at the two
397 most plausible drivers of change (temperature and precipitation, bottom plots Fig. 7) they do not
398 seem to be responsible for it. They both are affected by the El Niño event, when temperatures
399 increased and precipitation decreased; however, they do not show a contrasted sign on trends
400 before and after such an event. This leads to the hypothesis that the hydrological change
401 observed at these last stages of a glacier's life is independent of climatology. The most plausible
402 causes for this will be explained

403

404

405 4.3. Changes in the runoff-climate relationship

406 In this section, the runoff from temperature and precipitation is isolated in order to determine if
407 the observed hydrological dynamics are driven by climate or by shrinkage of the glacier. Figure 7
408 shows the mean monthly runoff for days with temperatures lower and higher than 2°C, i.e. water
409 yield series independent of temperature. Precipitation has also been added to the plot. It was
410 noted that water yield for days warmer than 2°C is significantly higher than water yield on days
411 cooler than 2°C. The characteristic evolution of runoff, with increasing amounts during most of
412 the study period up to mid-2016 and decreasing runoff from that point onwards was also
413 observed. The same evolution occurs for both days below and days above 2°C, and it occurs for
414 very similar amounts of precipitation. It seems evident, therefore, that flows from the melting
415 glacier are becoming less dependent on temperature, or climate in general, and more dependent
416 on the size of the glacier. Following the hypothesis of Section 1.2, regarding hydrological changes
417 of shrinking glaciers from 2013 to mid-2016, the runoff increases because glacier mass becomes
418 more sensitive to energy exchange as it gets smaller. From mid-2016 onwards, runoff decreases
419 because the water reservoir present in the ice has reached a threshold where its contribution
420 cannot be offset by incoming precipitation or potentially higher temperatures. The boxplots of Fig
421 8 (bottom) confirm this observation by showing water volumes significantly higher before than
422 after the breaking point, but also because the differences between water yield at < 2°C and water
423 yield at > 2°C are also smaller (and not significant) after the breaking point, indicating the
424 decreasing importance of temperature in the process of runoff production in the shrinking glacier

425

426

427



428 Finally, Figure 8 shows correlations between temperature/precipitation and monthly flows for
429 different time periods. In Figure 8a two years are compared that can be considered analogues in
430 terms of total flow (similar amounts of monthly flow, see Figure 6), but one year (2013-14) belongs
431 to the period of increasing flows due to deglaciation, before the 2016 breakpoint, and the other
432 year (2017) belongs to the period of decreasing flows after the breakpoint. Correlation between
433 temperature and flow is much higher ($R = 0.65$) for 2013-14 than for 2017 ($R = 0.35$), which would
434 corroborate the previous observation. However, precipitation also shows higher correlation with
435 flow for 2013-14 ($R = 0.67$) than for 2017 ($R = 0.42$), which would contradict the hypothesis. One
436 year, however, may not be representative of general trends, and so the same analysis is repeated,
437 not for individual years but for the whole periods pre- and post-2016 breakpoint (Fig. 8b). The
438 pattern seems more clear and corroborates the aforementioned hypothesis: correlation between
439 temperature and flow is significant for the pre-2016 period ($R = 0.55$) but is non-existent for the
440 post-2016 period ($R = -0.1$). Correlation between precipitation and flow is insignificant ($R = -0.23$)
441 for the pre-2016 period, and it is positive and significant for the post-2016 period ($R = 0.32$). These
442 previous observations lead to reasoning that during the years of hydrological monitoring (2013-
443 2017), the observed hydrological dynamic, with a marked break point in 2016, is a result of the
444 vanishing glacier process and not a response to climate variability.

445

446

5. Discussion and conclusions

447

448

449

450

451

452

453

454

455

456

457

458

459

460

461

462

463

464

465

466

467

468

469

470

471

472

473

474

475

476

477

478

479

480

481

482

483

The present paper shows a comprehensive analysis of the dynamics of an Andean glacier that is close to extinction, with special focus on its hydrological yield. We have benefited from a hydroclimatic monitoring network located in the surroundings of the glacier terminus that has been fully operative since 2013 and from monthly and annual estimations of mass balance and glacier extent respectively, derived from ice depth measurements and topographical surveys since 2006. Everything has been managed by the Institute of Hydrology Meteorology and Environmental Studies (IDEAM) of Colombia. The *Conejeras* glacier is currently an isolated small glacier that used to be part of a larger ice body called *Nevado de Santa Isabel*. Since measurements have been available, the glacier has constantly lost mass and, consequently, a reduction in its area is evident. The extinction of Colombian glaciers has been documented since 1850, with an average loss of 90% of their area, considering current values (IDEAM, 2012). This reduction, of about 3% per year, has been much larger during the last three decades (57%) compared to previous decades (23%), which is directly related to the general increase in temperatures in the region and to re-activation of volcanic activity (IDEAM, 2012; Rabatel et al., 2017). Since direct measurements began in 2006, our studied glacier has constantly lost area; however, until 2014 the area loss was gradual and restricted to the glacier front, and from 2014 the sharp retreat also involved higher parts of the glacier. The main reason for this strong shrinkage is the existence of above-zero temperatures during most of the year and less precipitation fallen as snow. This involves a constant migration of the equilibrium line to higher positions, and a decreasing albedo of the ice surface that involves greater energy absorption, the latter accelerated by intense activity of Nevado de el Ruiz in the last years. In terms of mass balance, very few months exhibit a gain of ice during the studied period and these tend to coincide with la Niña events (negative MEI episodes). These episodes cannot compensate for the great losses occurring during the majority of months, which are especially large during El Niño events (positive MEI episodes), when above-normal temperatures are recorded. The ENSO phenomenon exerts then great influence on the evolution of the glacier, similar to that reported for most inner tropical glaciers (Francou et al., 2004; Rabatel et al., 2013; Vuille et al., 2008); however, some episodes of great mass balance loss, such as that of 2014 (which coincides with the sharp decrease in glacier extent) cannot be explained by the ENSO. Observations of glacier surface during field surveys showed that during some periods of mass loss, surface ice retreat left ancient layers of volcanic ash exposed. The reduced energy reflectance caused by such ash layers might have triggered positive feedback that led to increasing melting and large ice retreat.

Glacier retreat is a worldwide phenomenon currently linked to global warming (IPCC, 2013). Amongst the environmental issues related to glacier retreat, the issue concerning water resources has produced a vast amount of research. This is because glaciers constitute water reservoirs in the form of accumulated ice over thousands of years, and they provide water supply to downstream areas for the benefit of life, ecosystems and human societies. The rapid decrease in



484 glacier extent during the last decades involves a change in water availability in glacier-dominated
485 regions and thus changes in water policies and water management are advisable (Huss, 2011;
486 Kundzewicz et al., 2008). In the short term, glacier retreat involves increasing runoff in
487 downstream areas but, after reaching a peak, runoff will eventually decrease until the contribution
488 of the glacier melt is zero when the glacier completely disappears. From a global perspective,
489 such a tipping point is referred to as *peak water* and has given rise to concern from the scientific
490 community (Gleick and Palaniappan, 2010; Huss and Hock, 2018; Kundzewicz et al., 2008; Mark
491 et al., 2017; Sorg et al., 2014). Research regarding the occurrence of such a runoff peak related
492 to glacier retreat demonstrates that it will not occur concurrently worldwide. In some mountain
493 areas it has already occurred, i.e. the Peruvian Andes (Baraer et al., 2012), the Western U.S
494 mountains (Frans et al., 2016), or Central Asia (Sorg et al., 2012). At the majority of studied
495 glacier basins it is expected to occur in the course of the present century (Immerzeel et al., 2013;
496 Ragettli et al., 2016; Sorg et al., 2014; Soruco et al., 2015). In recent global-scale research, Huss
497 and Hock (2018) state that in nearly half of the 56 large-scale glacierized drainage basins studied,
498 the peak water has already occurred. In the other half, it will occur in the next decades, depending
499 on extension of the ice cover fraction.

500 It was not the aim of this study to allocate such a tipping point in our studied glacier; however,
501 observations on the characteristics of streamflow along the studied period suggest that it may
502 have occurred during our study period. Our observations corroborate glacier melt being the main
503 contributor to runoff in the catchment. However, even when correlations between runoff and
504 temperature are mostly significant, the values are not as high as could be expected for a
505 glacierized catchment. This is due to a decreasing dependence of runoff on temperature, and
506 therefore to glacier melt, as at a certain point during the study period. We observed a changing
507 dynamic in most hydrological indicators, with a turning point in mid-2016, whereas climate
508 variables, i.e. temperature and precipitation, do not show such evident variation (besides the
509 exceptional conditions during an El Niño event). Both the PCA analysis and the monthly
510 aggregation of hydrological indices point to a less glacier-induced hydrological yield once the
511 runoff peak of 2016 was reached. According to literature (see Section 1.2.) this change from
512 increasing to decreasing runoff and to lesser importance of glacier contribution to total water yield
513 must be expected in glacierized catchments with glaciers close to extinction. The short length of
514 our hydrological series (five years) does not allow long-term analysis to determine water yield in
515 years of less deglaciation (i.e. from 2006 to 2012, see Fig. 3), which could verify or refute such a
516 hypothesis. However, when we isolated total runoff from climate variables before and after the
517 2016 breakpoint. (Figures 8 and 9), we observed that the increase and later decrease of flows
518 was mostly independent of temperature and precipitation, which would involve a glacier-driven
519 hydrological change. Summarizing, streamflow measured at the glacier's snout showed the
520 following characteristics: increasing trend in flow volume until mid-2016 and decreasing trend
521 thereafter: increasing diurnal variability (given by the range between high flows and low flows and
522 by the slope of the rising flow limb) up to mid-2016 and decreasing thereafter; decreasing and
523 increasing monthly variability (given by the coefficient of variation of flows within a given month)
524 before and after such date; high dependence of flow on temperatures before 2016 and low or null
525 dependence after 2016, with increasing dependence on precipitation. As well, this is supported
526 by an evident change in the type of hydrograph, from a prevalence of days with melt-driven
527 hydrographs (low baseflows, sharp melting pulse and great difference between high flows and
528 low flows) before 2016, to an increase in the occurrence of days with less influence of melt and
529 more influence by precipitation. All these characteristics support the idea of a hydrological change
530 driven by the deglaciation of the catchment, as summarized by Hock et al. (2005, see section
531 1.2). Data on glacierized area fraction supports this idea: the area covered by ice changed from
532 56-51% of the catchment in the 2006-2014 timespan to 39-35% of the catchment in 2015-2017;
533 therefore, the contribution of ice melt to total flow compared to that of precipitation must
534 necessarily decrease. This observation cannot be taken conclusively, because the time period of
535 hydrological observation is not long enough to deduce long-term trends and to explore
536 hydrological dynamics before the great decline in glacier extent in 2014. However, given the
537 current reduced size of the glacier (14 hectares, which represents 35% of the catchment that
538 drains into the gauge station), it is likely that water yield will continue to decrease in the upcoming
539 years, until glacier contribution ends and runoff depends only on the precipitation that falls within



540 the catchment. Like this glacier, other small glaciers in Colombia are expected to disappear in the
541 coming decades (Rabatel et al., 2017); thus, a similar hydrological response can be expected.

542 Unlike glaciers in the western semi-arid slopes of the Andes (i.e. Peru, Bolivia), Colombian
543 glaciers do not constitute the main source of freshwater for downstream populations (IDEAM,
544 2012). The succession of humid periods provides enough water in mountain areas, most of which
545 is stored in the deep soils of *Páramos*. These wetland ecosystems are mainly fed by rainfall (the
546 contribution of glacier melt is mostly unknown, IDEAM, 2012) and act as water buffers, ensuring
547 water availability during not-so-humid periods. Therefore, the role of glaciers in Colombia
548 regarding water resources, including our studied ice body, is more marginal, and the occurrence
549 of the *peak water* from glacier melt is not a current concern, as it is in Peru or Bolivia (Francou et
550 al., 2014). Yet this does not diminish relevance to our results because our observations may be
551 taken as an example of what can happen to the hydrology of glacierized basins in the tropics
552 whose glaciers are in the process of disappearing. Our studied glacier has a very small size
553 compared to other ice bodies in the region. This makes it respond rapidly to variations in climate,
554 as well as involving a rapid hydrological response of the catchment to the loss of ice, as was
555 observed in this work. The increasing/decreasing flow dynamic observed as the glacier retreated
556 occurred in roughly five years, and this is most likely related to the reduced size of our studied
557 glacier. Most studies on the hydrological response to glacier retreat consider large river basins
558 with large glacier coverage, usually by modeling approaches (i.e. Huss and Hock, 2018;
559 Immerzeel et al., 2013; Ragettli et al., 2016; Sorg et al., 2014, 2012; Stahl et al., 2008), and the
560 response times reported on either increasing flow at the initial stages or decreasing flow at the
561 final stages are always on the scale of decades. Our work demonstrates the necessity for in situ
562 observations on a finer scale in order to improve accuracy on future estimations of water
563 availability related to glacier retreat.

564

565 **Acknowledgments**

566 This work has been possible thanks to the monitoring network installed by the Department of
567 Ecosystems of the Colombian Institute for Hydrology, Meteorology and Environmental Studies
568 (*Instituto de Hidrología, Meteorología y Estudios Ambientales*, IDEAM) and to the monthly field
569 surveys on the Conejeras glacier and Río Claro river basin done by employed staff. Our sincere
570 gratitude to them, with special thanks to Yina Paola Nocua. The following projects gave economic
571 support to this paper: “*Estudio hidrológico de la montaña altoandina (Colombia) y su respuesta a*
572 *procesos de cambio global*” financed by Banco Santander, through the program of exchange
573 scholarships for young researchers in Ibero-America “*Becas Iberoamérica Jóvenes Profesores e*
574 *Investigadores* (2015); and CGL2017- 82216-R (HIDROIBERNIEVE) funded by the Spanish
575 Ministry of Economy and Competitiveness.

576

577

578

579

580 **6. References**

- 581 Baraer, M., Mark, B. G., McKenzie, J. M., Condom, T., Bury, J., Huh, K.-I., Portocarrero, C.,
582 Gómez, J. and Rathay, S.: Glacier recession and water resources in Peru's Cordillera Blanca, J.
583 Glaciol., 58(207), 134–150, doi:10.3189/2012JoG11J186, 2012.
- 584 Beniston, M.: Impacts of climatic change on water and associated economic activities in the
585 Swiss Alps, J. Hydrol., 412–413, 291–296, doi:10.1016/J.JHYDROL.2010.06.046, 2012.
- 586 Bradley, R. S., Vuille, M., Diaz, H. F. and Vergara, W.: Climate change. Threats to water
587 supplies in the tropical Andes., Science, 312(5781), 1755–6, doi:10.1126/science.1128087,
588 2006.
- 589 Cayan, D. R., Dettinger, M. D., Kammerdiener, S. A., Caprio, J. M., Peterson, D. H., Cayan, D.
590 R., Dettinger, M. D., Kammerdiener, S. A., Caprio, J. M. and Peterson, D. H.: Changes in the



- 591 Onset of Spring in the Western United States, *Bull. Am. Meteorol. Soc.*, 82(3), 399–415,
592 doi:10.1175/1520-0477(2001)082<0399:CITOOS>2.3.CO;2, 2001.
- 593 Ceballos, J. L., Euscátegui, C., Ramírez, J., Cañon, M., Huggel, C., Haeberli, W. and Machguth,
594 H.: Fast shrinkage of tropical glaciers in Colombia, *Ann. Glaciol.*, 43, 194–201,
595 doi:10.3189/172756406781812429, 2006.
- 596 Chander, G., Markham, B. L. and Helder, D. L.: Summary of current radiometric calibration
597 coefficients for Landsat MSS, TM, ETM+, and EO-1 ALI sensors, *Remote Sens. Environ.*,
598 113(5), 893–903, doi:10.1016/J.RSE.2009.01.007, 2009.
- 599 Chavez, P. S.: An improved dark-object subtraction technique for atmospheric scattering
600 correction of multispectral data, *Remote Sens. Environ.*, 24(3), 459–479, doi:10.1016/0034-
601 4257(88)90019-3, 1988.
- 602 Chevallier, P., Pouyaud, B., Suarez, W. and Condom, T.: Climate change threats to
603 environment in the tropical Andes: glaciers and water resources, *Reg. Environ. Chang.*, 11(S1),
604 179–187, doi:10.1007/s10113-010-0177-6, 2011.
- 605 Dozier, J.: Spectral signature of alpine snow cover from the landsat thematic mapper, *Remote*
606 *Sens. Environ.*, 28, 9–22, doi:10.1016/0034-4257(89)90101-6, 1989.
- 607 Favier, V., Wagnon, P. and Ribstein, P.: Glaciers of the outer and inner tropics: A different
608 behaviour but a common response to climatic forcing, *Geophys. Res. Lett.*, 31(16), L16403,
609 doi:10.1029/2004GL020654, 2004.
- 610 Francou, B. and Pouyaud, B.: Metodos de observacion de glaciares en los Andes tropicales :
611 mediciones de terreno y procesamiento de datos : version-1 : 2004, [online] Available from:
612 [https://www.researchgate.net/profile/Bernard_Pouyaud/publication/282171220_Metodos_de_ob](https://www.researchgate.net/profile/Bernard_Pouyaud/publication/282171220_Metodos_de_ob_servacion_de_glaciares_en_los_Andes_tropicales_mediciones_de_terreno_y_procesamiento_de_datos_version-1_2004/links/561ba9b808ae78721fa0f8ad.pdf)
613 [servacion_de_glaciares_en_los_Andes_tropicales_mediciones_de_terreno_y_procesamiento](https://www.researchgate.net/profile/Bernard_Pouyaud/publication/282171220_Metodos_de_ob_servacion_de_glaciares_en_los_Andes_tropicales_mediciones_de_terreno_y_procesamiento_de_datos_version-1_2004/links/561ba9b808ae78721fa0f8ad.pdf)
614 [de_datos_version-1_2004/links/561ba9b808ae78721fa0f8ad.pdf](https://www.researchgate.net/profile/Bernard_Pouyaud/publication/282171220_Metodos_de_ob_servacion_de_glaciares_en_los_Andes_tropicales_mediciones_de_terreno_y_procesamiento_de_datos_version-1_2004/links/561ba9b808ae78721fa0f8ad.pdf) (Accessed 12 March 2018),
615 2004.
- 616 Francou, B., Vuille, M., Wagnon, P., Mendoza, J. and Sicart, J.: Tropical climate change
617 recorded by a glacier in the central Andes during the last decades of the twentieth century:
618 Chacaltaya, Bolivia, 16°S, *J. Geophys. Res.*, 108(D5), 4154, doi:10.1029/2002JD002959, 2003.
- 619 Francou, B., Vuille, M., Favier, V. and Cáceres, B.: New evidence for an ENSO impact on low-
620 latitude glaciers: Antizana 15, Andes of Ecuador, 0°28'S, *J. Geophys. Res.*, 109(D18), D18106,
621 doi:10.1029/2003JD004484, 2004.
- 622 Francou, B., Rabatel, A., Soruco, A., Sicart, J. E., Silvestre, E. E., Ginot, P., Cáceres, B.,
623 Condom, T., Villacis, M., Ceballos, J. L., Lehmann, B., Anthelme, F., Dangles, O., Gomez, J.,
624 Favier, V., Maisincho, L., Jomelli, V., Vuille, M., Wagnon, P., Lejeune, Y., Ramallo, C. and
625 Mendoza, J.: Glaciares de los Andes tropicales: víctimas del cambio climático, Comunidad
626 Andina, PRAA, IRD. [online] Available from:
627 <http://bibliotecavirtual.minam.gob.pe/biam/handle/minam/1686> (Accessed 22 February 2018),
628 2014.
- 629 Frans, C., Istanbuluoglu, E., Lettenmaier, D. P., Clarke, G., Bohn, T. J. and Stumbaugh, M.:
630 Implications of decadal to century scale glacio-hydrological change for water resources of the
631 Hood River basin, OR, USA, *Hydrol. Process.*, 30(23), 4314–4329, doi:10.1002/hyp.10872,
632 2016.
- 633 Gleick, P. H. and Palaniappan, M.: Peak water limits to freshwater withdrawal and use, *Proc.*
634 *Natl. Acad. Sci.*, 107(25), 11155–11162, doi:10.1073/pnas.1004812107, 2010.
- 635 Hock, R., Jansson, P. and Braun, L. N.: Modelling the Response of Mountain Glacier Discharge
636 to Climate Warming, in *Global Change and Mountain Regions (A State of Knowledge*
637 *Overview)*, pp. 243–252, Springer, Dordrecht., 2005.
- 638 Huggel, C., Ceballos, J. L., Pulgarín, B., Ramírez, J. and Thouret, J.-C.: Review and
639 reassessment of hazards owing to volcano–glacier interactions in Colombia, *Ann. Glaciol.*, 45,
640 128–136, doi:10.3189/172756407782282408, 2007.



- 641 Huss, M.: Present and future contribution of glacier storage change to runoff from macroscale
642 drainage basins in Europe, *Water Resour. Res.*, 47(7), doi:10.1029/2010WR010299, 2011.
- 643 Huss, M. and Hock, R.: Global-scale hydrological response to future glacier mass loss, *Nat.*
644 *Clim. Chang.*, 8(2), 135–140, doi:10.1038/s41558-017-0049-x, 2018.
- 645 IDEAM: Glaciares de Colombia, más que montañas con hielo, edited by Comité de
646 Comunicaciones y Publicaciones del IDEAM, Bogotá., 2012.
- 647 Immerzeel, W. W., Pellicciotti, F. and Bierkens, M. F. P.: Rising river flows throughout the
648 twenty-first century in two Himalayan glacierized watersheds, *Nat. Geosci.*, 6(9), 742–745,
649 doi:10.1038/ngeo1896, 2013.
- 650 IPCC: Climate Change 2013: The Physical Science Basis. Contribution of Working Group I to
651 the Fifth Assessment Report of the Intergovernmental Panel on Climate Change, edited by T. F.
652 Stocker, D. Qin, G.-K. Plattner, M. Tignor, S. K. Allen, J. Boschung, A. Nauels, Y. Xia, V. Bex,
653 and P. M. Midgley, Cambridge University Press, Cambridge, United Kingdom and New York,
654 NY, USA., 2013.
- 655 Kaser, G. and Omaston, H.: Tropical glaciers, Cambridge University Press. [online] Available
656 from: https://books.google.es/books?hl=es&lr=&id=ZEB-I3twN_gC&oi=fnd&pg=PR11&dq=tropical+glaciers&ots=WLwn1fdjig&sig=897EG6q4Pyc113vo9Qb2bnyUo7g#v=onepage&q=tropical+glaciers&f=false (Accessed 21 November 2017), 2002.
- 659 Kaser, G., Grosshauser, M. and Marzeion, B.: Contribution potential of glaciers to water
660 availability in different climate regimes., *Proc. Natl. Acad. Sci. U. S. A.*, 107(47), 20223–7,
661 doi:10.1073/pnas.1008162107, 2010.
- 662 Kundzewicz, Z. W., Mata, L. J., W., A. N., Döll, P., Jimenez, B., Miller, K., Oki, T., Şed, Z. and
663 Shiklomanov, I.: The implications of projected climate change for freshwater resources and their
664 management, *Hydrol. Sci. J.*, 53(1), 3–10, doi:10.1623/hysj.53.1.3, 2008.
- 665 López-Moreno, J. I., Fontaneda, S., Bazo, J., Revuelto, J., Azorin-Molina, C., Valero-Garcés, B.,
666 Morán-Tejeda, E., Vicente-Serrano, S. M., Zubieta, R. and Alejo-Cochachín, J.: Recent glacier
667 retreat and climate trends in Cordillera Huaytapallana, Peru, *Glob. Planet. Change*, 112, 1–11,
668 doi:10.1016/j.gloplacha.2013.10.010, 2014.
- 669 López-Moreno, J. I., Valero-Garcés, B., Mark, B., Condom, T., Revuelto, J., Azorin-Molina, C.,
670 Bazo, J., Frugone, M., Vicente-Serrano, S. M. and Alejo-Cochachin, J.: Hydrological and
671 depositional processes associated with recent glacier recession in Yanamarey catchment,
672 Cordillera Blanca (Peru), *Sci. Total Environ.*, 579, 272–282,
673 doi:10.1016/J.SCITOTENV.2016.11.107, 2017.
- 674 Mark, B. G., French, A., Baraer, M., Carey, M., Bury, J., Young, K. R., Polk, M. H., Wigmore, O.,
675 Lagos, P., Crumley, R., McKenzie, J. M. and Lutz, L.: Glacier loss and hydro-social risks in the
676 Peruvian Andes, *Glob. Planet. Change*, 159, 61–76, doi:10.1016/J.GLOPLACHA.2017.10.003,
677 2017.
- 678 Mölg, N., Ceballos, J. L., Huggel, C., Micheletti, N., Rabatel, A. and Zemp, M.: Ten years of
679 monthly mass balance of Conejeras glacier, Colombia, and their evaluation using different
680 interpolation methods, *Geogr. Ann. Ser. A, Phys. Geogr.*, 99(2), 155–176,
681 doi:10.1080/04353676.2017.1297678, 2017.
- 682 Padró, J.-C., Pons, X., Aragonés, D., Díaz-Delgado, R., García, D., Bustamante, J., Pesquer,
683 L., Domingo-Marimon, C., González-Guerrero, Ó., Cristóbal, J., Doktor, D. and Lange, M.:
684 Radiometric Correction of Simultaneously Acquired Landsat-7/Landsat-8 and Sentinel-2A
685 Imagery Using Pseudoinvariant Areas (PIA): Contributing to the Landsat Time Series Legacy,
686 *Remote Sens.*, 9(12), 1319, doi:10.3390/rs9121319, 2017.
- 687 Poveda, G. and Pineda, K.: Reassessment of Colombia's tropical glaciers retreat rates: are they
688 bound to disappear during the 2010–2020 decade?, *Adv. Geosci.*, 22, 107–116,
689 doi:10.5194/adgeo-22-107-2009, 2009.
- 690 Poveda, G., Waylen, P. R. and Pulwarty, R. S.: Annual and inter-annual variability of the
691 present climate in northern South America and southern Mesoamerica, *Palaeogeogr.*



- 692 Palaeoclimatol. Palaeoecol., 234(1), 3–27, doi:10.1016/j.palaeo.2005.10.031, 2006.
- 693 Rabatel, A., Francou, B., Soruco, A., Gomez, J., Cáceres, B., Ceballos, J. L., Basantes, R.,
694 Vuille, M., Sicart, J.-E., Huggel, C., Scheel, M., Lejeune, Y., Arnaud, Y., Collet, M., Condom, T.,
695 Consoli, G., Favier, V., Jomelli, V., Galarraga, R., Ginot, P., Maisincho, L., Mendoza, J.,
696 Ménégos, M., Ramirez, E., Ribstein, P., Suarez, W., Villacis, M. and Wagnon, P.: Current state
697 of glaciers in the tropical Andes: a multi-century perspective on glacier evolution and climate
698 change, *Cryosph.*, 7(1), 81–102, doi:10.5194/tc-7-81-2013, 2013.
- 699 Rabatel, A., Ceballos, J. L., Micheletti, N., Jordan, E., Braitmeier, M., González, J., Mölg, N.,
700 Ménégos, M., Huggel, C. and Zemp, M.: Toward an imminent extinction of Colombian glaciers?,
701 *Geogr. Ann. Ser. A, Phys. Geogr.*, 1–21, doi:10.1080/04353676.2017.1383015, 2017.
- 702 Ragetli, S., Immerzeel, W. W. and Pellicciotti, F.: Contrasting climate change impact on river
703 flows from high-altitude catchments in the Himalayan and Andes Mountains., *Proc. Natl. Acad.*
704 *Sci. U. S. A.*, 113(33), 9222–7, doi:10.1073/pnas.1606526113, 2016.
- 705 Ribstein, P., Tiriau, E., Francou, B. and Saravia, R.: Tropical climate and glacier hydrology: a
706 case study in Bolivia, *J. Hydrol.*, 165(1–4), 221–234, doi:10.1016/0022-1694(94)02572-S, 1995.
- 707 Sicart, J. E., Hock, R., Ribstein, P., Litt, M. and Ramirez, E.: Analysis of seasonal variations in
708 mass balance and meltwater discharge of the tropical Zongo Glacier by application of a
709 distributed energy balance model, *J. Geophys. Res.*, 116(D13), D13105,
710 doi:10.1029/2010JD015105, 2011.
- 711 Sorg, A., Bolch, T., Stoffel, M., Solomina, O. and Beniston, M.: Climate change impacts on
712 glaciers and runoff in Tien Shan (Central Asia), *Nat. Clim. Chang.*, 2(10), 725–731,
713 doi:10.1038/nclimate1592, 2012.
- 714 Sorg, A., Huss, M., Rohrer, M. and Stoffel, M.: The days of plenty might soon be over in
715 glacierized Central Asian catchments, *Environ. Res. Lett.*, 9(10), 104018, doi:10.1088/1748-
716 9326/9/10/104018, 2014.
- 717 Soruco, A., Vincent, C., Rabatel, A., Francou, B., Thibert, E., Sicart, J. E. and Condom, T.:
718 Contribution of glacier runoff to water resources of La Paz city, Bolivia (16° S), *Ann. Glaciol.*,
719 56(70), 147–154, doi:10.3189/2015AoG70A001, 2015.
- 720 Stahl, K., Moore, R. D., Shea, J. M., Hutchinson, D. and Cannon, A. J.: Coupled modelling of
721 glacier and streamflow response to future climate scenarios, *Water Resour. Res.*, 44(2),
722 doi:10.1029/2007WR005956, 2008.
- 723 Stewart, I. T., Cayan, D. R. and Dettinger, M. D.: Changes in Snowmelt Runoff Timing in
724 Western North America under a 'Business as Usual' Climate Change Scenario, *Clim. Change*,
725 62(1–3), 217–232, doi:10.1023/B:CLIM.0000013702.22656.e8, 2004.
- 726 Vaughan, D. G., Comiso, J. C., Allison, I., Carrasco, J., Kaser, G., Kwok, R., Mote, P., Murray,
727 T., Paul, F., Ren, J., Rignot, E., Solomina, O., Steffen, K. and Zhang, T.: Observations:
728 Cryosphere, in *Climate Change 2013: The Physical Science Basis. Contribution of Working*
729 *Group I to the Fifth Assessment Report of the Intergovernmental Panel on Climate Change*,
730 edited by T. F. Stocker, D. Qin, G.-K. Plattner, M. Tignor, S. K. Allen, J. Boschung, A. Nauels,
731 Y. Xia, V. Bex, and P. M. Midgley, pp. 317–382, Cambridge University Press, Cambridge,
732 United Kingdom and New York, NY, USA., 2013.
- 733 Vuille, M., Francou, B., Wagnon, P., Juen, I., Kaser, G., Mark, B. G. and Bradley, R. S.: Climate
734 change and tropical Andean glaciers: Past, present and future, *Earth-Science Rev.*, 89(3–4),
735 79–96, doi:10.1016/J.EARSCIREV.2008.04.002, 2008.
- 736 Vuille, M., Carey, M., Huggel, C., Buytaert, W., Rabatel, A., Jacobsen, D., Soruco, A., Villacis,
737 M., Yarleque, C., Timm, O. E., Condom, T., Salzmann, N. and Sicart, J.-E.: Rapid decline of
738 snow and ice in the tropical Andes – Impacts, uncertainties and challenges ahead, *Earth-*
739 *Science Rev.*, 176, 195–213, doi:10.1016/j.earscirev.2017.09.019, 2017.
- 740
- 741



780 **Table 1.** Hydrologic and climatic indices computed from the hourly streamflow, temperature and
781 precipitation series. * *hpulse* is computed as the hourly equivalent of the melting-runoff spring
782 pulse proposed by Cayán et al. (2001) for daily data, i.e.: the time of the day when the minimum
783 cumulative streamflow anomaly occurs, which is equivalent to finding the hour after which most
784 flows are greater than the daily average.

Index	Explanation	unit
<i>totalQ</i>	total daily water yield	m ³ day ⁻¹
<i>Qmax</i>	value of maximum hourly water yield per day	m ³ hour ⁻¹
<i>hpulse</i> *	hour of the day when the melting streamflow pulse starts	hour of the day
<i>Qbase</i>	mean water yield value between the start of the day (00:00 h) and the hour when <i>hpulse</i> occurs	m ³ hour ⁻¹
<i>hQmax</i>	hour of the day when	hour of the day
<i>Qrange</i>	difference between <i>Qbase</i> and <i>Qmax</i>	m ³ hour ⁻¹
<i>Qslope</i>	slope of the streamflow rising limb between <i>hpulse</i> and <i>hQmax</i>	slope in %
<i>decayslope</i>	slope of the streamflow decaying limb between <i>hQmax</i> and 23:00h	slope in %
<i>Tmax</i>	value of maximum hourly temperature per day	°C hour ⁻¹
<i>Tmin</i>	value of minimum hourly temperature per day	°C hour ⁻¹
<i>Tmed</i>	mean daily temperature	°C day ⁻¹
<i>Trange</i>	difference between <i>Tmin</i> and <i>Tmax</i>	°C hour ⁻¹
<i>hTmax</i>	hour of the day when the <i>Tmax</i> occurs	hour of the day
<i>Diffth</i>	time difference between <i>hTmax</i> and <i>hQmax</i>	Hours
<i>Pmax</i>	value of maximum hourly precipitation per day	mm hour ⁻¹
<i>hPmax</i>	hour of the day when the <i>Pmax</i> occurs	hour of the day
<i>pp</i>	daily precipitation sum	mm day ⁻¹

785

786

787

788 **Table 2.** Pearson correlation coefficient between daily hydrological indices and temperature for
789 days with and without precipitation (left) and for days only without precipitation (right) between
790 July 2013 and June 2017. The correlation values correspond to the average obtained by 100
791 resampling iterations (n = 99) of the correlation test. * and ** indicate that correlations are
792 significant at 95% and 99% confidence respectively (two-tailed test).

793

Index	days with and without precipitation (n = 99)				days without precipitation (n = 99)			
	<i>Tmin</i>	<i>Tmax</i>	<i>Tmed</i>	<i>Trange</i>	<i>Tmin</i>	<i>Tmax</i>	<i>Tmed</i>	<i>Trange</i>
<i>total</i>	0.25**	0.12	0.19	0.02	0.31**	0.54**	0.53**	-0.39**
<i>Qmax</i>	0.25**	0.30**	0.33**	-0.18	0.24*	0.64**	0.57**	-0.54**
<i>Qbase</i>	0.13	-0.13	-0.05	0.22*	0.18	0.05	0.11	0.06
<i>Qrange</i>	0.25**	0.36**	0.37**	-0.25**	0.22*	0.65**	0.58**	-0.57**
<i>Qslope</i>	0.18	0.40**	0.38**	-0.34**	0.12	0.58**	0.48**	-0.55**
<i>hQmax</i>	0.06	-0.03	0.00	0.06	0.04	0.00	0.02	0.02
<i>Hpulse</i>	-0.18	-0.17	-0.21*	0.08	-0.36**	-0.50**	-0.52**	0.31**

794

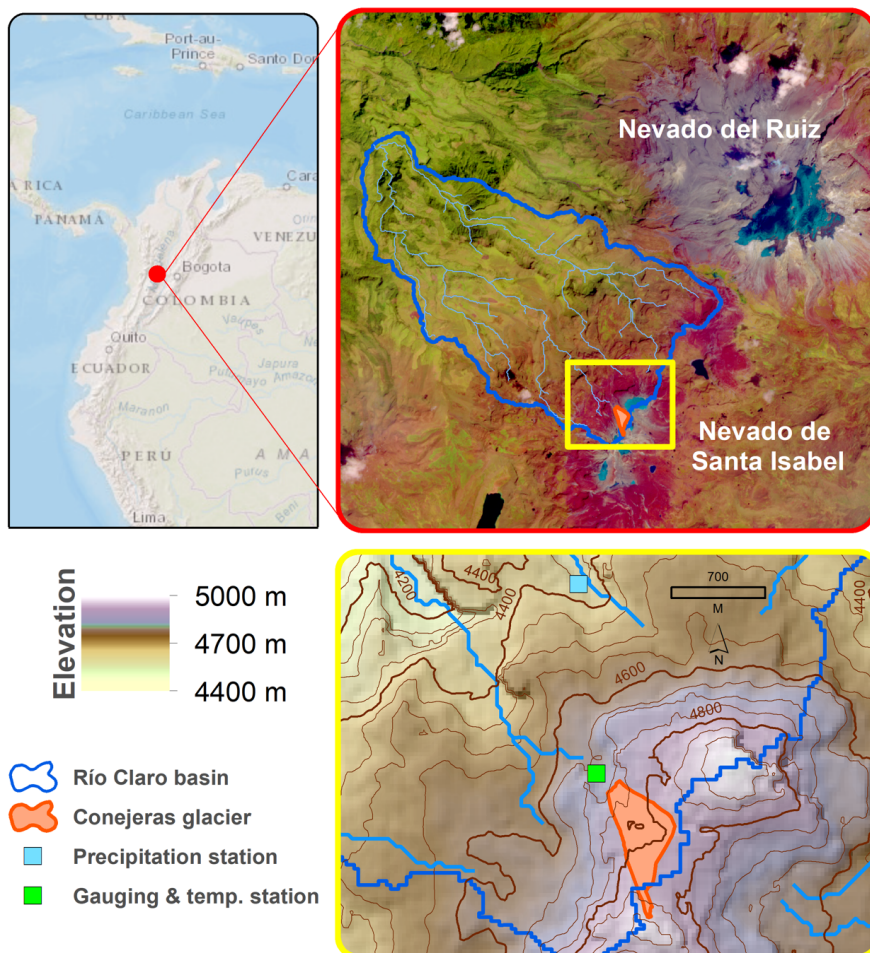
795

796 **Table 3.** Mean and standard deviation of variance explained (%) by each PC throughout the 25
797 bootstrapped samples

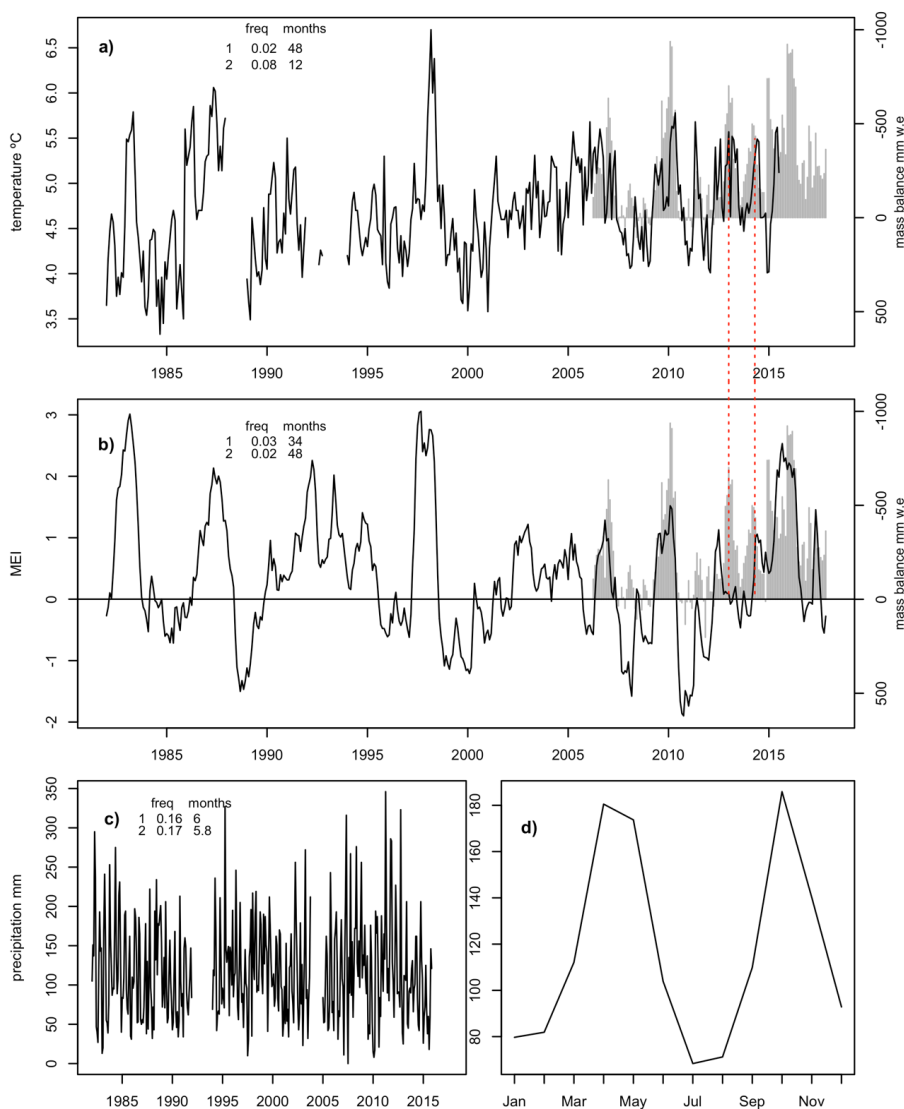
PC	Mean	standard deviation
PC1	47.78	5.91
PC2	34.99	5.66
PC3	11.82	6.77

798

799

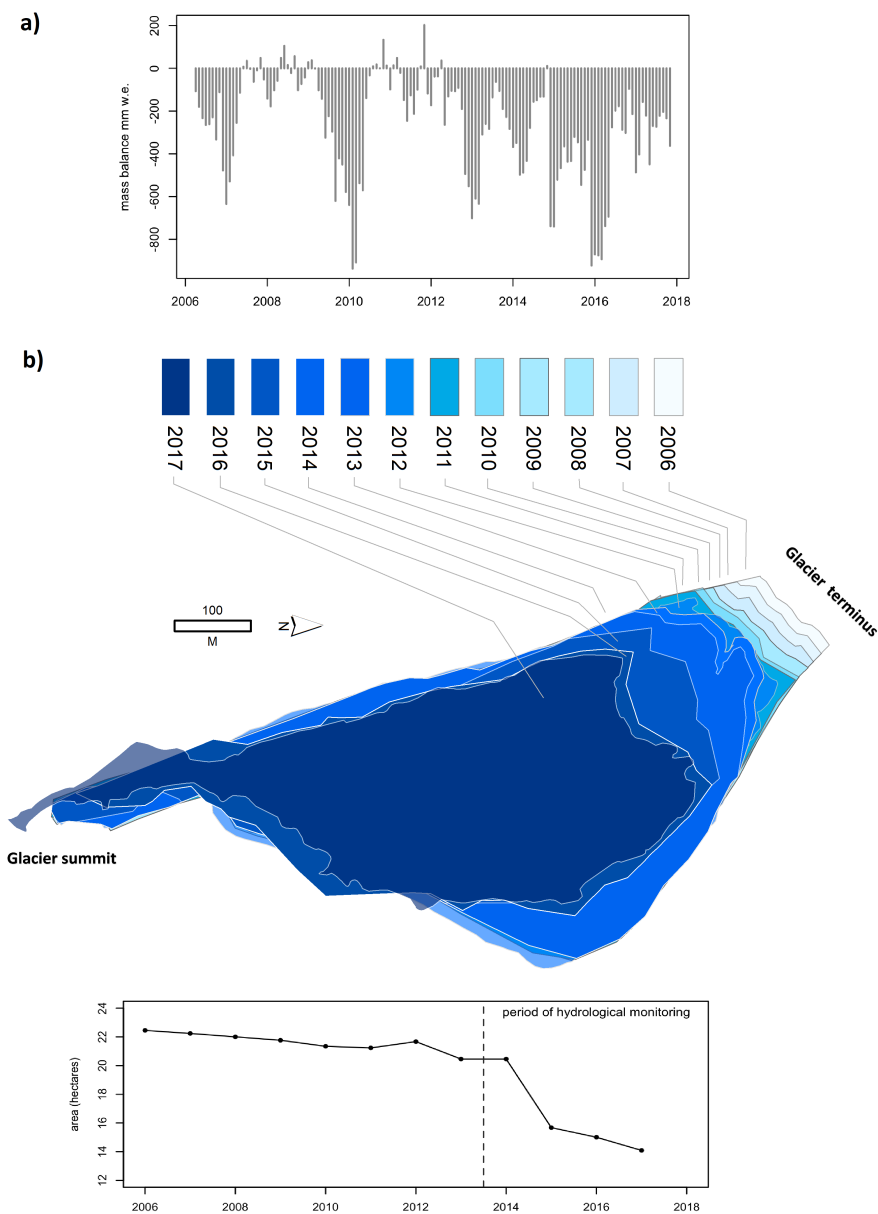


800
801 **Figure 1.** Study area, showing the glaciers of the Parque Nacional Natural de los Nevados, and
802 the Río Claro river basin (top map) and the Conejeiras glacier with hydro-meteorological stations
803 (bottom map).

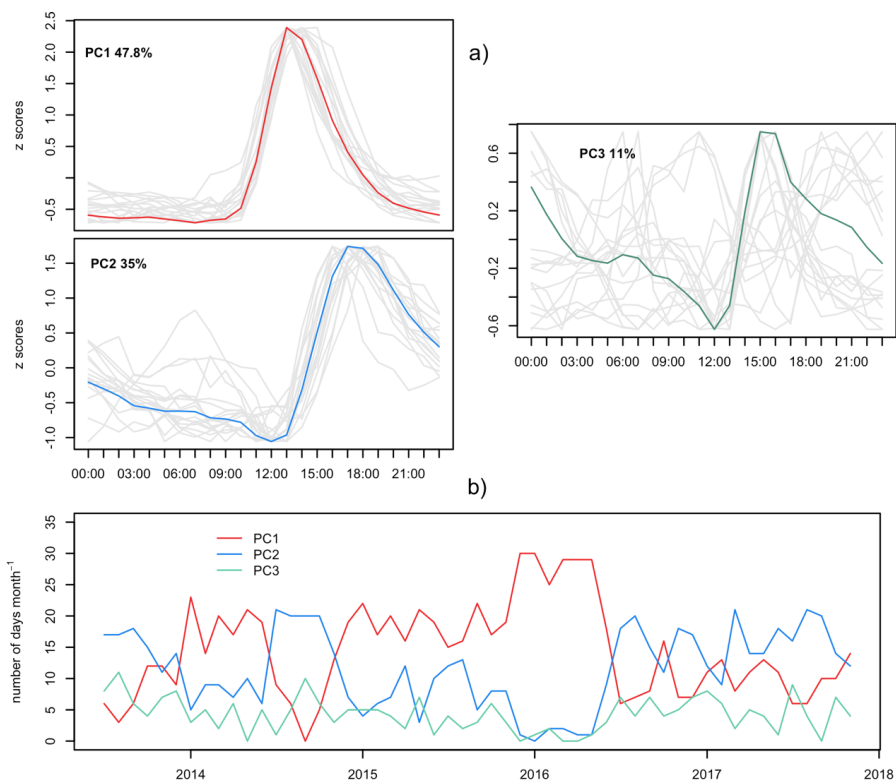


804

805 **Figure 2.** Long-term evolution of climate variables in the study area. a) monthly air temperature
 806 at the Brisas meteorological station (2721 m. asl), 1982-2015, and the Conejeras glacier's mass
 807 balance 2006-2018 (note the inverted axis in the latter); b) Multivariate ENSO Index, and the
 808 Conejeras glacier's mass balance (note the inverted axis in the latter); c) monthly precipitation at
 809 the Brisas station, 1982-2015; d) monthly long-term average of precipitation at the Brisas station.
 810 The frequency and its equivalent in months (1/frequency) of the two top spectral densities from
 811 spectral analysis is shown for temperature, MEI and precipitation monthly series. Red dashed
 812 lines indicate peak mass balance loss coincident with temperature peaks but not with MEI peaks.

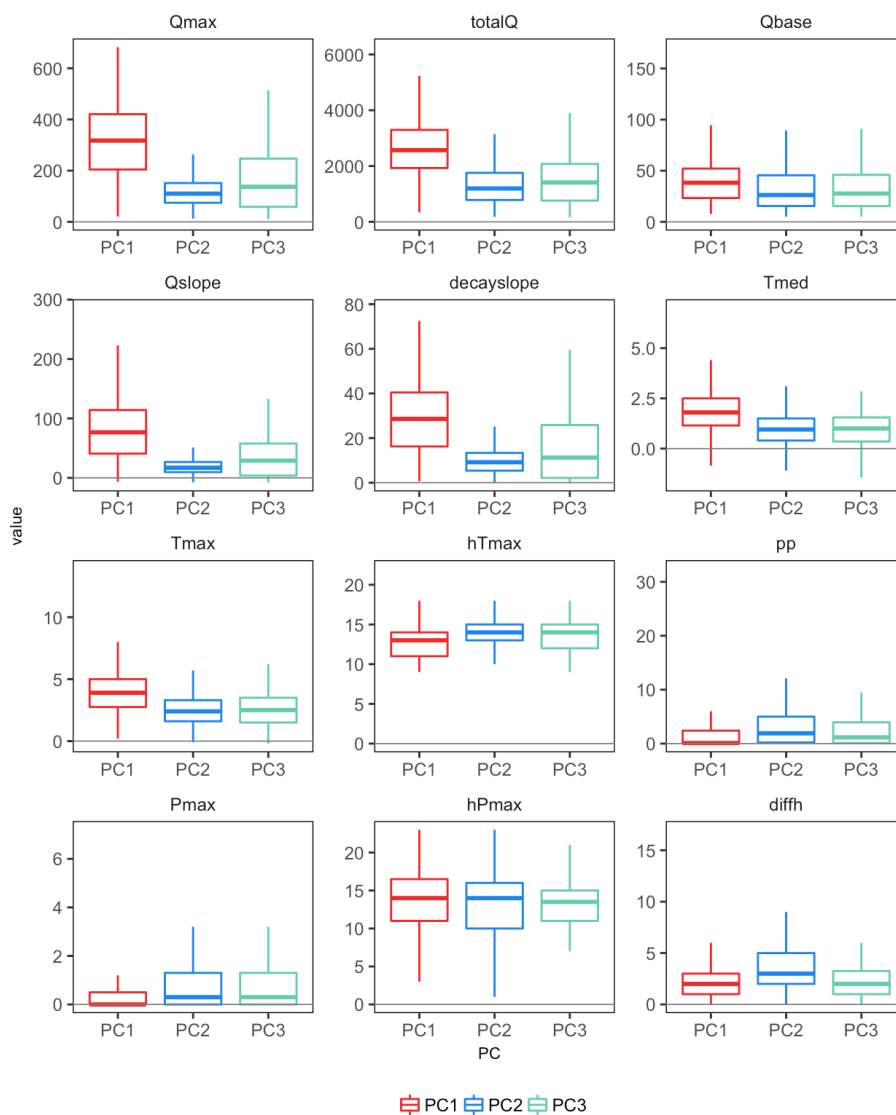


813
 814 **Figure 3.** Evolution of the Conejeras glacier. a) mass balance in mm w.e. b) extension in hectares.
 815
 816
 817
 818
 819



820

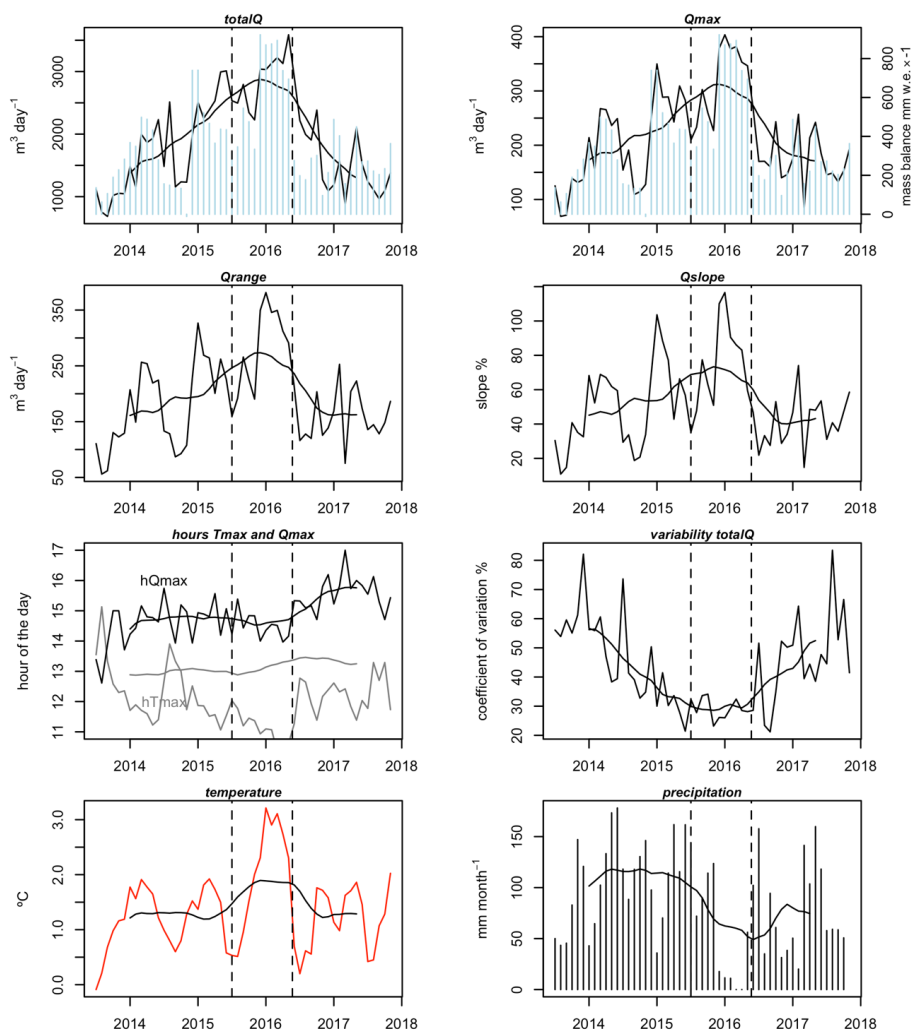
821 **Figure 4.** Principal Component Analysis on hourly streamflow. a) scores of the three main
822 principal components (patterns of daily streamflow), with gray lines indicating the scores for each
823 one of the 25 bootstrapped samples in the recursive PCA, and colored lines indicating the
824 average. b) Evolution of the number of days per month that show maximum correlation with each
825 PC. Red corresponds to PC1, blue corresponds to PC2 and green corresponds to PC3



826

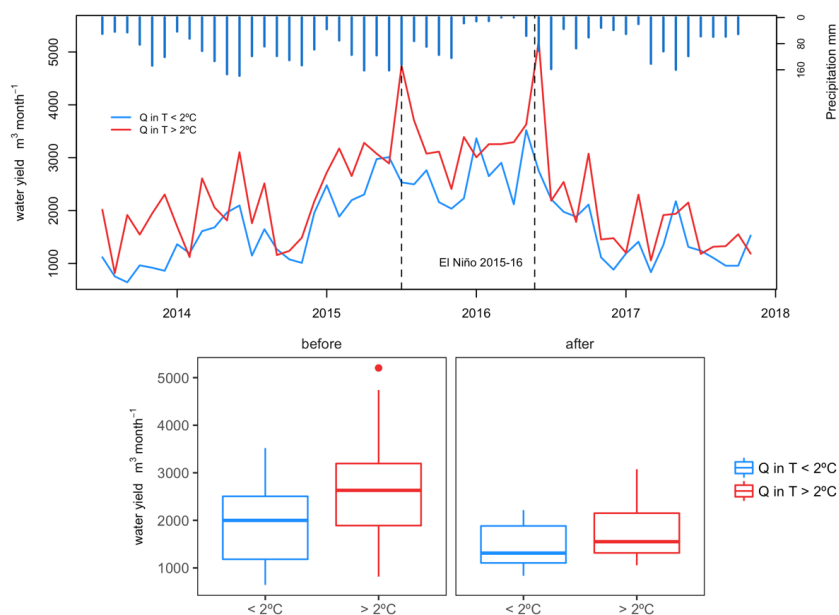
827 **Figure 5.** Summary of the frequency distributions (boxplots) of the hydrological and
 828 meteorological indicators for days grouped within PC1, PC2 and PC3.

829



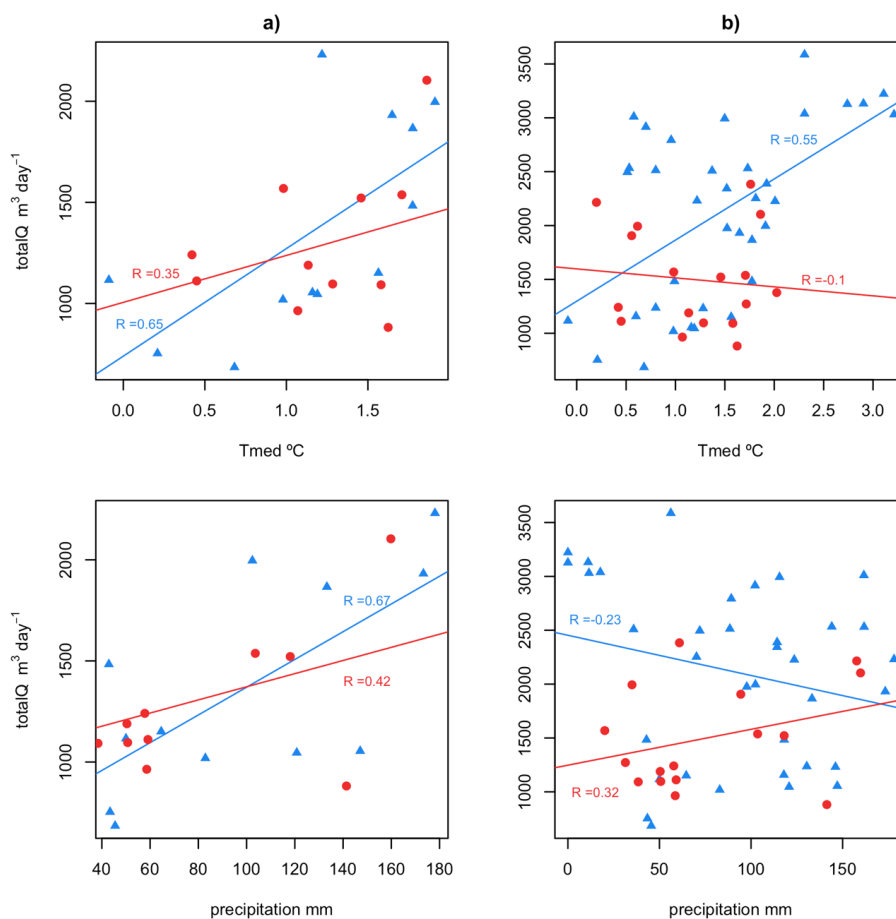
830
 831
 832
 833
 834
 835

Figure 6. Evolution of monthly averaged hydrological indices, temperature, precipitation and glacier mass balance (in blue bars on the top two plots), for the study period. Dashed lines indicate the 2015-2016 strong El Niño event. 12-months window moving average (black smooth lines) are shown to represent trends.



836

837 **Figure 7.** Mean monthly water yield (Q), for days with temperature lower than 2°C (blue) and
 838 days with temperature higher than 2°C (red) Top: Inter-annual evolution with indication of El Niño
 839 2015-16 event (grey shading), breakpoint in water yield evolution (dashed line), and monthly
 840 precipitation (blue bars); bottom: comparative boxplots for water yield before and after breakpoint
 841 in May 2016.



842

843 **Figure 8.** Correlations between monthly flow and monthly temperature (top plots) and
844 precipitation (bottom plots) for: a) 2013-14 (blue triangles) and 2017 (red circles) years, which are
845 considered as analogues in terms of amounts of flow; and b) months before May 2016 breakpoint
846 (blue triangles) and months after May 2016 breakpoint (red circles).

847